

# CERES TRMM-PFM-VIRS Edition2A SSF Cloud Properties - Accuracy and Validation

This section discusses the spectral radiances and cloud parameters associated with the SSF data set version Edition2A. The cloud parameters in the SSF are the result of convolving the values for the clear-sky and cloudy data derived for each 2-km VIRS pixel within a CERES footprint. (See [Spatial matching of imager properties and broadband radiation](#).) Consult the [SSF Collection Guide](#) for information on how clear sky and cloud data are stored on the SSF product. Additional details of the validation process and some of the algorithm changes associated with Edition2A are given in the [September 19, 2001 telecon presentation \(PDF\)](#).

Five radiances taken at 0.67, 1.6, 3.7, 10.8, and 12.0  $\mu\text{m}$ , channels 1 through 5, respectively, are measured for each VIRS pixel. Based on the values of these radiances, each VIRS pixel is classified as clear, cloudy, bad data, or no retrieval. Each clear or cloudy pixel is categorized as weak or strong to indicate the degree of confidence in the selection. Clear pixels can also have an additional classifier, either snow, aerosol, smoke, fire, sunglint, or shadow. The cloudy pixels can also have a sunglint sub-classification meaning that they were detected at angles favorable for the viewing of specular reflection from the surface. Atmospheric profiles of temperature, ozone, and humidity, model estimates of surface skin temperature (see [MOA description](#)), elevation, and one of the twenty surface types ([CERES Surface Properties Home Page](#)) are also associated with each VIRS pixel.

The 10.8- $\mu\text{m}$  surface skin temperature is computed for each clear pixel while the following values are computed for each cloudy pixel: phase (ice or water), visible (0.67  $\mu\text{m}$ ) optical depth, infrared (10.8  $\mu\text{m}$ ) emissivity, liquid or ice water path  $WP$ , effective droplet radius  $r_e$  or effective ice crystal diameter  $D_e$ , cloud-top pressure, effective cloud height and temperature, and cloud-base pressure. Nominally, cloud phase and effective particle sizes are computed separately using the 1.6- and 3.7- $\mu\text{m}$  channels. However, only the 3.7- $\mu\text{m}$  results are included in Edition2A.

The bad-data pixels are those having at least one radiance that was set to a default value or out of the allowed range. The greatest problem causing bad data was the saturation of the thermal channels over land. The saturation temperatures for the VIRS Version 5 are 321.4, 324.9, and 319.4 K for channels 3, 4, and 5, respectively. Because of its relatively low maximum temperature and its reflected solar component, the 3.7- $\mu\text{m}$  channel was often saturated during midday over deserts and scrubland. To acquire as many clear pixels as possible, it was assumed that saturated 3.7- $\mu\text{m}$  pixels over land or desert were actually clear if there was no saturation in the other channels and the 10.8- $\mu\text{m}$  temperature was greater than 300 K. The 3.7- $\mu\text{m}$  temperature was set to the maximum temperature. If these conditions were not met, then a bad data classification was assigned to the pixel. No-retrieval pixels are those that are initially identified as cloudy, but their radiances cannot be interpreted with the theoretical models used to derive cloud particle size and optical depth.

## VIRS Data

The cloud products rely on accurately calibrated imager radiances. VIRS Version 5 radiance data were used for Edition2A. The VIRS thermal infrared channels are calibrated with onboard blackbodies and the solar channels are calibrated approximately once per month using a solar-viewing diffuser. Space looks provide zero radiance levels for the calibrations. Barnes et al. (2000) and Lyu et al. (2000) summarize the operational VIRS calibrations. The nominal VIRS calibrations were compared to other calibrated satellite data to determine stability and relative gains to determine any inconsistencies with other commonly used imagers. During the period from January through August 1998 and March 2000, corresponding to times when the PFM operated continuously, the VIRS solar and infrared channels were linearly correlated with the CERES SW and LW radiances, respectively, taken each day over ocean, land, and desert areas separately using three solar zenith angle (SZA) ranges to produce a slope for each data category. A time series of these slopes was used to monitor any trends in the imager calibrations assuming stability in the CERES reference dataset. Differences between March 1998 and March 2000 were also used to determine long-term changes. It is assumed that the data taken over ocean are the most reliable because of the spectral homogeneity of the surface reflectance and temperature. The imagers were also compared to collocated and co-angled radiances from the eastern Geostationary Operational Environmental Satellite (GOES-8; continuous from Jan. 1998 - July 2000), the ERS-2 Along Track Scanning Radiometer (ATSR-2; two periods: Jan - Aug 1998 and Feb. - July 2000), and the MODIS Airborne Simulator (MAS; Jan. 25, 1999 over Amazon Basin) on the ER-2 aircraft. The GOES-8 was calibrated against the ATSR-2 on a monthly basis since 1995 to establish a trend line in the GOES gain. Thus, comparison of GOES and VIRS is equivalent to comparing ATSR-2 and VIRS over ocean for purposes of detecting long-term trends, because both VIRS and ATSR-2 use diffuser systems for calibrating their visible channels. Spectral differences were normalized for all of the imager comparisons. Except for the near-infrared gain changes, details of the calibration studies for each channel are given by Minnis et al. (2001). The following remarks summarize the basic findings.

**Ch. 1, VIS (0.64  $\mu\text{m}$ ):** No statistically significant trends were found in the VIRS data between 1998 and 2001 using the CERES and GOES-8/ATSR-2 comparisons.

**Ch. 2, NIR (1.62  $\mu\text{m}$ ):** After correcting for temperature variations of the detector (See [Aerosol Properties - Accuracy and Validation](#)), the NIR radiances  $L_2$  were corrected for contamination by thermal radiation at 5.2  $\mu\text{m}$  because of imperfections in the instrument filter. The corrected radiance is

$$L_2' = L_2 - DL_2,$$

where

$$DL2 = S2 * [-226.3 + 157.1*L4 - 304.9*(L4-L5) + 0.453*VZA - 0.0240*VZA^2] / 100,$$

$L2$ ,  $L4$ , and  $L5$  are the measured radiances for VIRS channels 2, 4, and 5, respectively, and  $S2$  is the solar constant for channel 2 ( $78.30 \text{ W m}^{-2} \mu\text{m}^{-1} \text{ sr}^{-1}$ ). The formula for  $DL2$  was developed empirically by Ignatov and Stowe (2000) and is in good agreement with theoretical estimates. This correction does not account for variations in the surface emissivity so that it may be in error by 10-15% over some surfaces resulting in an overall NIR radiance error of ~0.2%. This error is generally not significant except for possibly some low-reflectance scenes such as clear ocean.

In the comparisons with CERES shortwave radiances, no statistically significant trend in the gain was found during first 8 months for  $SZA < 45^\circ$  and for  $SZA > 60^\circ$ . A significant degradation in the gain of 1%/month was found for  $45^\circ < SZA < 60^\circ$ . However, the length of record does not eliminate the potential for a seasonal cycle. Comparison of the results from March 1998 and March 2000 do not support the trend. The channel-2 radiances were also correlated with matched data from corresponding channels on ATSR-2, MAS, and Terra MODIS using the following equations, where  $LA$ ,  $LM$ , and  $LT$  correspond to ATSR-2, MAS, and MODIS, respectively,  $G$  is the slope, and  $I$  is the offset.

$$\text{ATSR-2 NIR: } LA = G * L2' + I$$

$$1998: G = 1.171; \quad I = 0.000; \quad N = 392.$$

$$2000: G = 1.168; \quad I = 0.000; \quad N = 130.$$

$$\text{MAS NIR: } LM = G * L2' + I$$

$$1999: G = 1.215 \quad I = 0 \quad N = 114.$$

$$\text{Terra MODIS: } LT = G * L2' + I$$

$$2000-01: G = 1.157; \quad I = -0.198 \text{ correlations from 4 months}$$

In this instance, the results from MODIS and ATSR-2 are very consistent and supported by the MAS results. Given these results and those of Lyu et al. (2000), it is concluded that there is no significant trend in the VIRS NIR gain. The large gain differences between VIRS and the other imagers are supported by a comparison of cloud droplet sizes retrieved using channels 2 and 3. The NIR-derived particle sizes were much larger than their 3.8- $\mu\text{m}$  counterparts using the nominal calibration but were in excellent agreement using the ATSR-2 gains. Thus, it was concluded that additional correction must be applied to the NIR radiance. The values used here are

$$L2'' = 1.17 L2'$$

This quantity was used to calculate the mean NIR radiance for each SSF pixel. Details of the determination of the 1.6- $\mu\text{m}$  channel correction are given by Young et al. (2001).

**Ch. 3, SIR (3.78  $\mu\text{m}$ ):** No trends were detected using CERES data.

**Ch. 4, IR (10.75  $\mu\text{m}$ ) and Ch. 5, WS (11.95  $\mu\text{m}$ ):**

No statistically significant trend in either the IR or SWC calibrations was found through comparisons with CERES, GOES, and MODIS. However, a day-night change in the brightness temperature difference between channels 4 and 5 was found for low temperature pixels ( $T < 235 \text{ K}$ ). This difference appears to be due to solar heating of the spacecraft because the variation in the diurnal difference is highly correlated with the TRMM beta angle. It is not clear if this diurnal difference is due to changes in the calibration of either channel or to changes in both channels. The nighttime calibration appears to be the correct one. The change averages 0.7 K for pixels with  $T < 238 \text{ K}$ , but may be as 1.0 K at certain times. This variation does not appear to affect warmer pixel readings. For more details, see Minnis et al. (2001).

## BAD DATA DAYS

April 25 and 26, 1998 are days known to have mostly bad data. Any results for these days should be used with caution.

## Cloud Parameters

Preliminary assessment of the uncertainties in some of the cloud parameters has been completed. Many other datasets must be compared with the CERES VIRS cloud analyses before final error numbers are assigned. The cloud parameters have been evaluated visually by comparing a large number of high-resolution images with pictures of derived cloud products over a selected number of regions to ensure that the results appear to be qualitatively consistent with the imagery. Some of the parameters have been compared with climatological values to obtain a rough quantitative evaluation. The results have also been averaged for various surface types and angular ranges to determine any systematic variability. The most quantitative evaluations use estimates of similar quantities derived from passive and active radiometric measurements at surface sites, in particular, the ARM Southern Great Plains (SGP) facility in central Oklahoma. The available results have been compared with the Edition2A quantities and are being documented with a paper currently in preparation. The results are similar to those

found applying the CERES algorithm to GOES-8 data.

**Cloud amount** - Figure 1 shows the comparison of mean zonal cloud amounts from VIRS for July 1998 and from surface observations for the period from 1971 - 1996. The VIRS zonal means are within  $\pm 1.5\%$  of the climatological values from the surface. The results in Fig. 1 demonstrate that the retrievals from CERES are reasonable as do the image evaluations. More quantitative direct comparisons with coincident surface observations, both subjective and objective will be used to provide a more quantitative assessment of the cloud amount uncertainties.

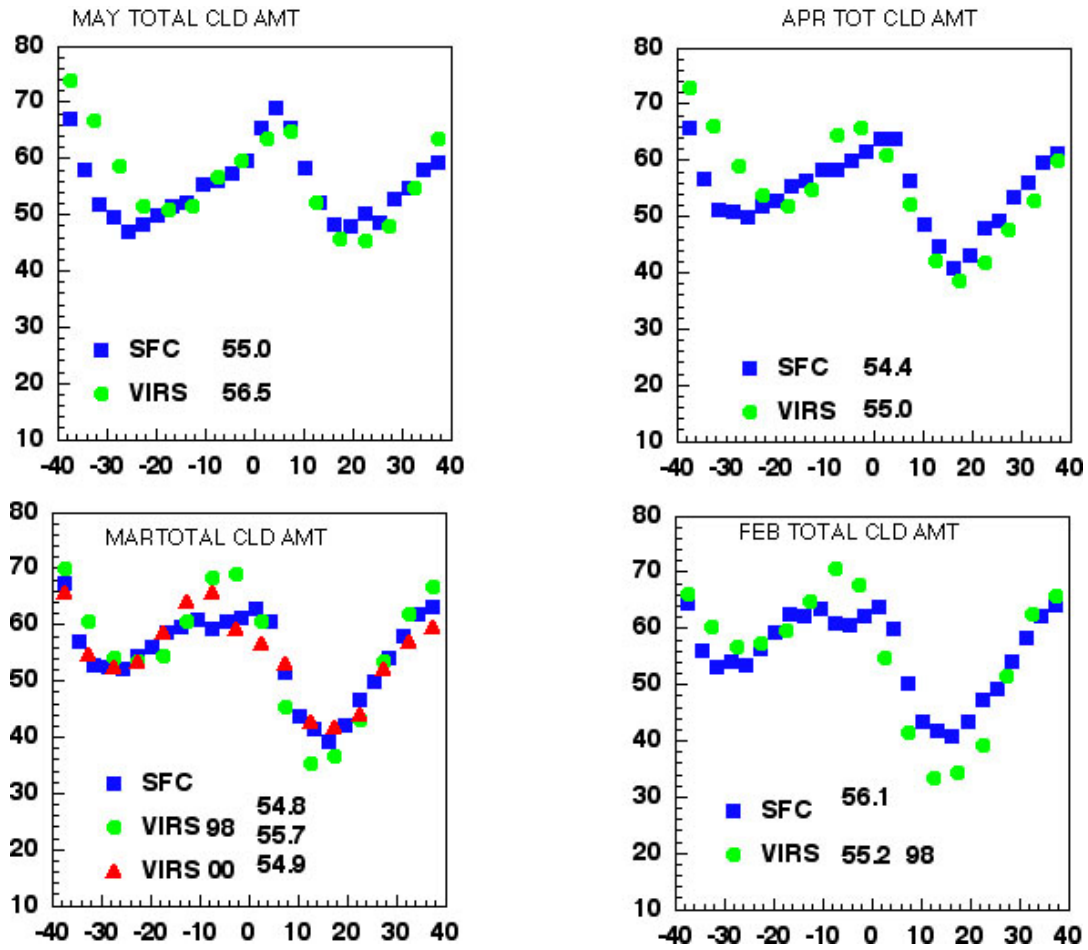


Figure 1. Comparison of monthly mean cloud fraction from surface observations for 1971-1992 to VIRS retrievals for 1998 and 2000.

**Cloud phase** - This parameter is more difficult to evaluate because it requires either in situ or combinations of passive and active remote sensing data. Inspection of the results with coincident imagery indicates that, during the daytime, the cirrus clouds, even very thin ones, are generally identified as ice clouds. The edges of these clouds are occasionally classified as water clouds and the very thin cirrus over low clouds are sometimes classified as water clouds. At night, the phase classification is less reliable except when the cloud temperature is  $< 233\text{K}$  (ice) or  $> 273\text{K}$  (liquid). The daytime fraction of ice clouds from VIRS relative to the total for January through July 1998 is 1.0% less than the mean value derived long-term (1971-1996) surface observations (Hahn et al. 1999) where cirrus and cumulonimbi are assumed to be ice clouds. Future assessments of cloud phase will use direct comparisons with remotely sensed data from the surface.

**Cloud height, pressure, temperature** - These parameters are all related because the cloud temperature is used to ascertain cloud height and the height is used to select the pressure. Effective cloud height derived from VIRS should be an altitude somewhere between the top and base of the cloud. It corresponds to the mean radiating temperature of the cloud. For water clouds, the mean radiating temperature is usually within a few 100 m of the top. For cirrus clouds, it can be close to the cloud base or near cloud top depending on the density of the cloud. Comparisons with the radar observations over the ARM southern Great Plains (SGP) site, summarized in Table 1 for cloud height and temperature, are reported in detail by Dong et al. (2001a). Uncertainties in cloud-top pressure can be determined from the altitude differences in Table 1. During both daytime and nighttime, the effective cloud height is always between the mean and the top altitudes derived from the surface data where the mean is average of the top and base from the radar data. The one exception is for thin clouds ( $\tau < 5$ ) during the daytime. In those cases, the average VIRS effective cloud height was below the mean height, but above the base height as determined from the surface. In three cases for the daytime thin clouds, the effective cloud height was actually below the base and, in one instance was above the top height. During the daytime, several stratus cloud effective heights exceeded the radar cloud-top altitude. However, the temperatures were within 1 K of that determined from the surface sounding. This height error is due to the low resolution of the input profiles of temperature used by CERES. Boundary layer inversions were often not sufficiently resolved in the numerical weather analyses. To avoid this inversion problem over ocean, CERES uses a lapse-rate method instead of a vertical profile of temperature to convert temperature to altitude. To test the lapse-rate method, the CERES algorithm was used to estimate cloud height from Geostationary Operational Environmental Satellite (GOES) data over the southeastern Pacific where strong temperature inversions occur and the numerical weather analysis profiles generally do not sufficiently characterize the inversions. The comparisons showed that the altitudes derived with the CERES lapse-rate technique yield

cloud heights that are typically within about 300 m of the cloud base or top (Garreaud et al. 2000). Thus, the problems encountered over the SGP site for boundary-layer stratus are diminished over ocean.

At night, the mean effective cloud heights for liquid water and ice clouds are 0.6 km higher than their daytime counterparts. This difference is probably due to real diurnal changes in the vertical structure of clouds, but it also includes the differences in thin cloud height retrievals between day and night seen in Table 1. The nighttime method relies entirely on thermal channels, while the daytime algorithm uses both visible and thermal channels. The impact of a low cloud underneath a high cloud on the derived height is much greater during daylight because the low cloud adds to the optical depth, the parameter used to determine emissivity. At night, the surface and low-cloud temperatures are similar so that the optical depth, which relies on the cloud-top and surface temperature difference, is less sensitive to multilayered clouds. Thus, in areas where thin cirrus is prevalent over scattered low clouds or deserts where the surface emissivity is uncertain, the mean effective cloud heights are considerably greater than their daytime counterparts. Users should be aware of this day-night difference in cloud height. Previous methods have used a single channel infrared temperature to assign cloud heights at night resulting gross underestimates for optically thin clouds. This approach represents an improvement over the single-channel technique.

**Cloud optical depth, effective particle size** - These parameters were also evaluated by Dong et al. (2001a) using retrievals of the same quantities from surface-based instruments at the ARM site using the techniques of Dong et al. (1997) and Mace et al. (1998). Nominally, only single-layered stratus and cirrus clouds were considered. However, some of the daytime cirrus cases were contaminated by low clouds. The surface-based cirrus retrieval method is limited to optically thin clouds and loses reliability for clouds thicker than 3 or visible optical depth. The cirrus comparisons must be performed with extreme caution because of the variability of cirrus and because of the effect of clouds underneath the cirrus. The optical depths derived from VIRS are restricted to roughly 10 or less at night because of the limitations of infrared retrievals. Thus, estimates of  $r_e$ ,  $\tau$  and  $LWP$  from VIRS at night should not be used except for optically thin clouds. Overall, the agreement between the two datasets is excellent during the daytime. Because the nighttime microphysical properties are limited, the agreement for stratus breaks down. Generally, the standard deviations during the daytime are within the CERES accuracy goals. The VIRS and surface daytime retrievals agree at roughly same level as a similar comparison of surface, aircraft, and GOES retrievals for stratus over the same site (Dong et al. 2001b). The GOES retrievals used for the CERES algorithm. The number of samples here is still too small for this one site. These results represent only one set of climatological conditions. Comparisons at the SGP and other sites should continue.

**Table 1: Uncertainties in cloud parameters based on comparisons at the ARM SGP site.**

		Mean difference (VIRS- ARM)	Standard deviation	Standard dev of difference (%)	N
<b>DAY</b>	Thin cloud temperature vs mean	11.8 K	11.7 K	-	18
	Thick cloud temperature vs mean	-6.8 K	8.2 K	-	41
	Thin cloud height vs. mean	-1.1 km	1.7 km	-	18
	Thin cloud height vs. top	-2.1 km	2.0 km	-	18
	Thick cloud height vs. mean	0.4 km	1.3 km	-	41
	Thick cloud height vs. top	-0.4 km	1.6 km	-	41
	Stratus optical depth	-1.5	6.2	21	25
	Stratus Effective radius	0.7	1.8 $\mu\text{m}$	20	25
	Liquid water path	-18 $\text{gm}^{-2}$	41 $\text{gm}^{-2}$	35	25
	Cirrus optical depth	0.7	1.3	38	7
	Cirrus effective diameter	0.5 $\mu\text{m}$	17.0 $\mu\text{m}$	72	7
	Ice water path	4.3 $\text{gm}^{-2}$	18.3 $\text{gm}^{-2}$	49	7
<b>NIGHT</b>	Thin cloud temperature vs mean	-1.6 K	9.5 K	-	49
	Thick cloud temperature vs mean	-6.4 K	7.3 K	-	31
	Thin cloud height vs. mean	0.7 km	1.4 km	-	49
	Thin cloud height vs. top	-0.5 km	1.5 km	-	49
	Thick cloud height vs. mean	1.6 km	1.1 km	-	31
	Thick cloud height vs. top	-0.5 km	1.0 km	-	31
	Stratus optical depth	-20.9	21.4	67	22
	Stratus Effective	0.7 $\mu\text{m}$	2.7 $\mu\text{m}$	33	22

	radius ( $\mu\text{m}$ )			
Cirrus optical depth	0.6	1.1	78	16
Cirrus effective diameter ( $\mu\text{m}$ )	-16.8 $\mu\text{m}$	20.0 $\mu\text{m}$	32	16
Ice water path	2.0 $\text{gm}^{-2}$	27.5 $\text{gm}^{-2}$	97	16

## Angular Dependencies

VIRS on TRMM provides the first opportunity to evaluate the angular dependencies of cloud properties without a location bias. Imagers previously used to derive cloud properties have been either geo- or sun-synchronous so that the viewing and illumination conditions were always dependent on the Earth location. Because of its precessing orbit, the TRMM allows the VIRS to view the same location at nearly all available SZAs over the course of 46 days or less from a variety of VZAs and relative azimuth angles (RAZ). However, the VIRS is limited in VZA to  $48^\circ$  and only views regions between  $37^\circ\text{N}$  and  $37^\circ\text{S}$ .

The mean cloud properties for March 1998 are presented as functions of VZA and SZA in Figs. 2 and 3, respectively. Only daytime data are shown in Fig. 2 except for Fig. 2d, which has cloud amounts for day and night. The trends in these figures are typical for other months. Effective droplet size increases by an average of 8% over ocean and only 1% over land over the  $48^\circ$  of VZA, while  $D_e$  only rises by 2.5% or less (Fig. 2a). Water cloud optical depths decrease by 14% and 3.6%, respectively over ocean and land, while  $\tau$  for ice clouds is invariant over ocean, but decreases by 11% over land. Mean cloud height is essentially constant with VZA. Cloud amount is separated into daytime and nighttime determinations as indicated by D and N, respectively, in Fig. 2d. Nighttime cloud amounts are less than their daytime counterparts by no more than 1% for  $VZA < 10^\circ$ . Mean cloud amount increases with VZA in a relative sense by 12% during the daytime and by 2% at night. This day-night difference is due VZA-dependent thresholds that were introduced to minimize the VZA dependence of cloud fraction that normally arises because of foreshortening of the scene by the sides of clouds (e.g., Minnis 1989). This minimization effort, which was introduced to obtain similar cloud property statistics at each VZA, involves a tradeoff of partially cloud-filled or extremely thin cloud pixels between the clear and cloudy categories. Both VIS and IR VZA-dependent thresholds were applied, but the IR threshold is the more dominant of the two. Hence, some of the broken or thin low clouds that were detected with the VIS threshold during the daylight hours were probably missed with the IR threshold that was designed primarily to account for very thin cirrus clouds. Thus, the day-night difference in cloud fraction seen in Fig. 2d arose because of these thresholds. Users should be aware of this threshold artifact.

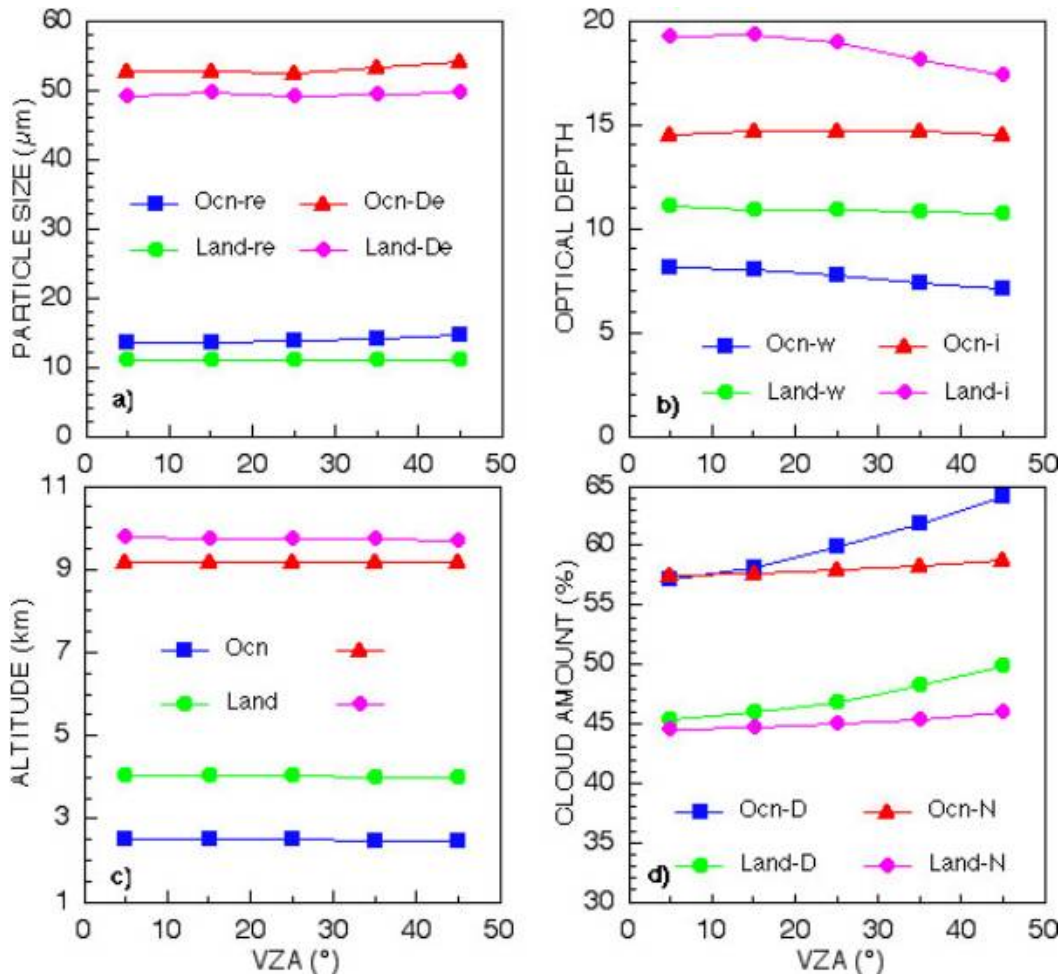


Fig. 2. VZA dependence of mean cloud properties from VIRS during March 1998.

Because of sampling issues, the values for SZA < 25° should be ignored for purposes of studying the SZA effect. Cloud droplet size decreases with SZA (increases with  $\mu_0$ , the cosine of SZA), an effect opposite that for VZA. In Fig. 3a,  $r_e$  drops by 21% and 25% between SZAs of 25° and 78° over ocean and land, respectively. Part of the decrease, especially over land may be due to actual changes in cloud properties or to some residual bias due to smaller SZAs occurring more frequently over the rain forests where  $r_e$  is a maximum over land. A closer examination of this dependence for other months supports this idea in that decrease in  $r_e$  over the range of SZA is 15% over land during boreal summer. Thus, the observed variation in  $r_e$  with SZA should be viewed as a combination of both retrieval artifacts, due to the illumination of cloud sides and other 3-D effects not taken into account with the plane-parallel models, and real changes in clouds as they develop convectively or over different regions. The relative contributions of these two phenomena are subjects for further study. Ice cloud particle sizes very much less with SZA, decreasing by 6 and 9% over ocean and land, respectively. Cloud optical depth (Fig. 3b) shows the opposite behavior with a substantial increase with SZA (decrease with increasing  $\mu_0$ ). For water clouds,  $\tau$  increases by factors of 1.7 and 2.5, respectively, over ocean and land. The ice cloud optical depths increase, on average, by 28% over both surface types. Again, these changes in  $\tau$  are due to both morphological effects and diurnal variations in the clouds. For example,

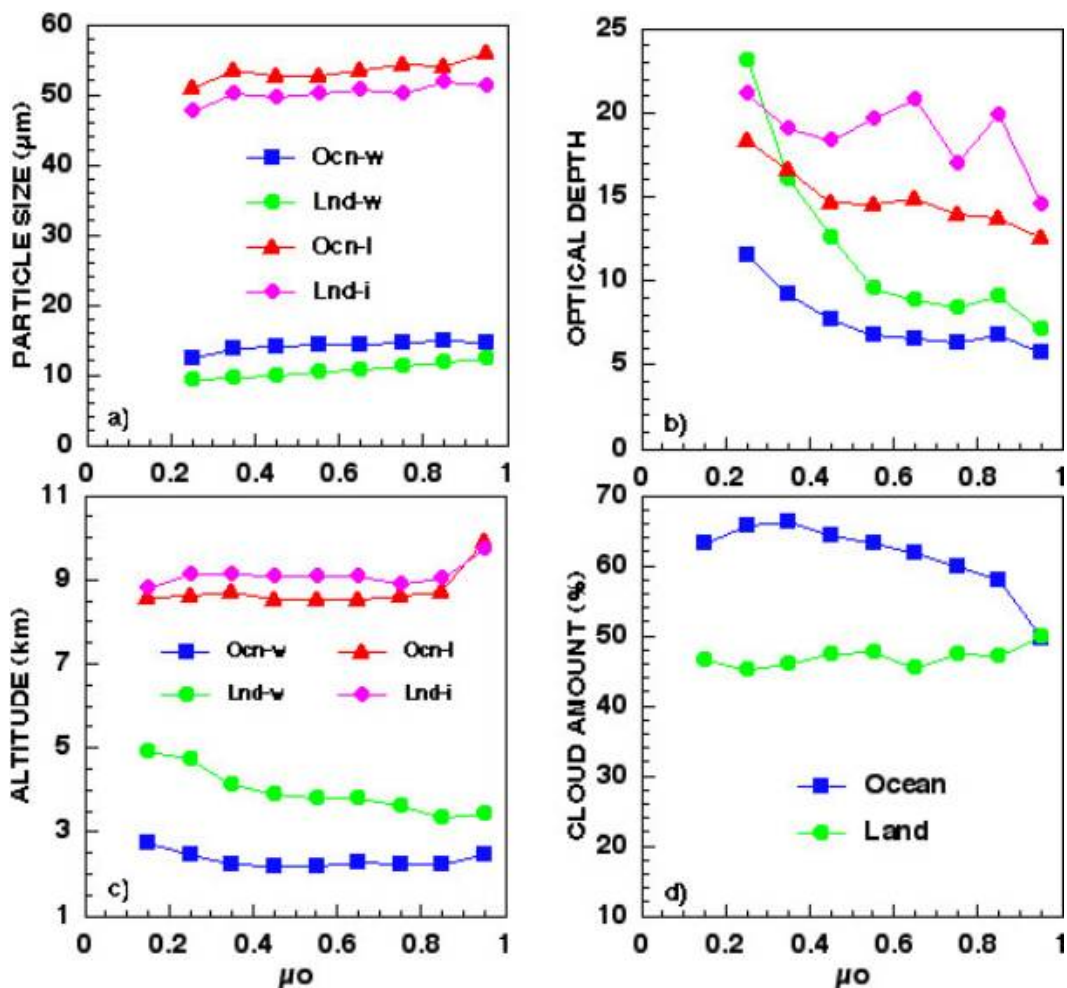


Fig. 3. SZA dependence of mean cloud properties from VIRS during March 1998.

stratus clouds, which dominate the water cloud coverage over the oceans, tend to dissipate during the daytime and reform during the late afternoon, a behavior that would produce the type of variation seen here. Convective cloud generation is also diurnally driven with late afternoon or nighttime deep convective development occurring over most land areas. Diurnal cycles in optical depth would suggest similar variations in cloud height. Neglecting the first and last points because of sampling and methodology issues, the water cloud heights increase by 1.4 and 0.2 km, on average, Figure 3c indicates that liquid water cloud heights increase with SZA over both land and water by 1.4 and 0.2 km, respectively. Ice cloud heights show no significant dependence on SZA. Mean cloud fraction is relatively constant with SZA over land, but increases by 11% at  $\mu_0 = 0.25$  relative to the value at  $\mu_0 = 0.85$  over ocean. This result is consistent with the diurnal cycle of marine stratus, but suggests that on average, the various diurnal variations in cloud fraction over land are balanced over 24 hours by including all regions.

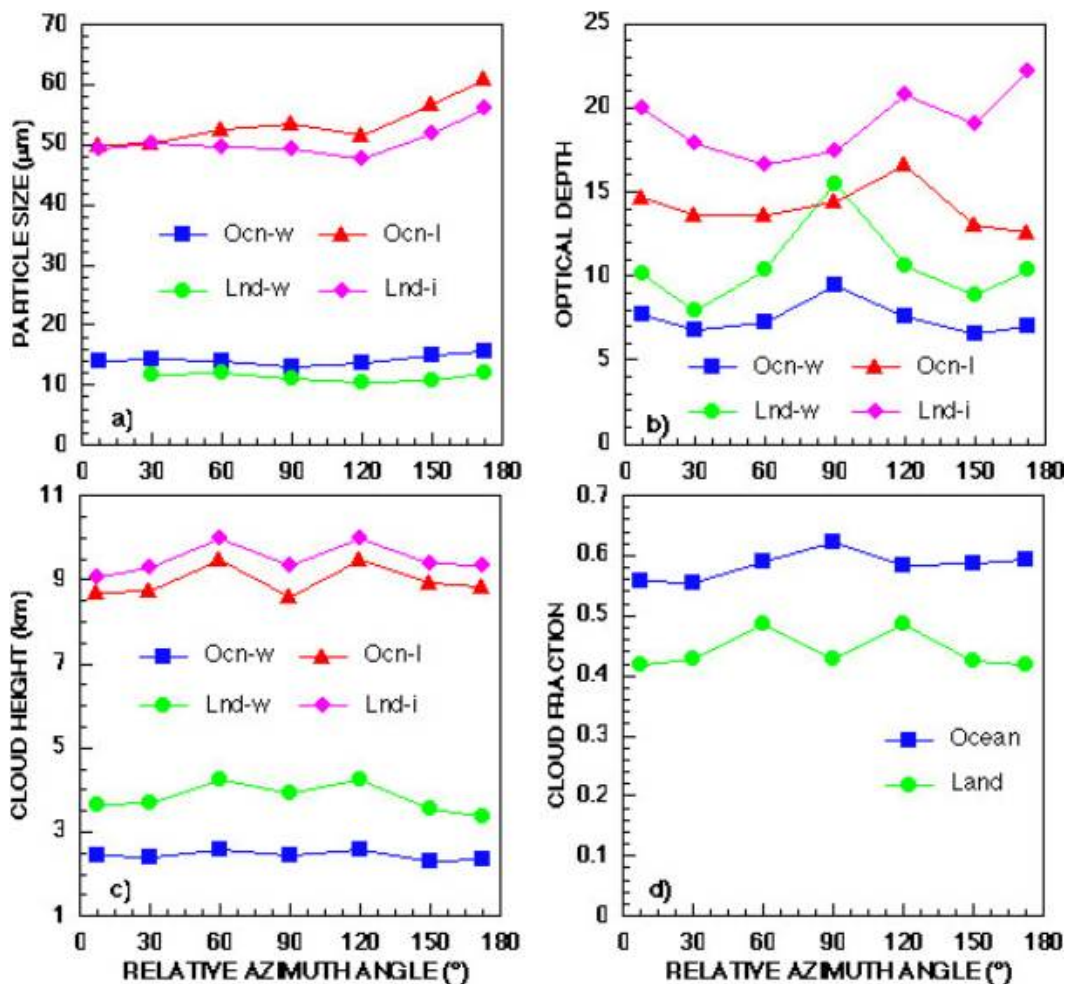


Fig. 4. RAZ dependence of mean cloud properties from VIRS during March 1998.

Cloud amounts also vary with relative azimuth angle as shown in Fig. 4. In this case, however, there appears to be some variation of location and, perhaps, SZA with RAZ because cloud fraction (Fig. 4d) and cloud height (Fig. 4c) are quite variable unlike the relatively smooth changes seen for the other angles. The variability also changes with month indicating that more than one season would be needed to study the RAZ dependence. Some generalities can be obtained from the current datasets, however. The maxima in  $D_e$  and  $r_e$  (Fig. 4a) occur in the backscatter direction for all months. For 9 months of VIRS data, the mean difference between the maximum and minimum average values of both particles sizes is 21%. Because distinctly different phase functions are used for both phases, this maximum in the backscatter direction is most likely due to 3-D effects in the clouds. The variations of cloud optical depth in Fig. 4b are not necessarily typical of those seen during other months. During some periods, the maximum occurs in backscattering direction and sometimes at other angles. The average ranges in mean optical depth over 180° of RAZ are 35% and 27% for water and ice clouds, respectively. It is clear from these results that any RAZ dependence must be taken into account as a function of the SZA and VZA.

Overall, the angle dependencies show that the derived cloud properties are reasonable at a level of 25% or better. More likely, the values are consistent at a higher level of accuracy because of the natural variability that occurs in clouds but is reflected in the angular dependencies (i.e., the SZA-diurnal variation, the RAZ-location variation). The VZA dependencies in cloud optical depth and cloud particle size are probably mostly due to the increase in cloud fraction with VZA. More optically thin or broken clouds are detected at higher VZAs resulting in a decrease of the mean  $\tau$ , which in turn would cause an apparent increase in the effective particle size. The ice crystal phase functions for CERES yield results that appear to be as representative as the water cloud phase functions because the variations of  $D_e$  with any particular angle are no worse than the variations in  $r_e$ . This result is consistent with the findings of Chepfer et al. (2001).

Return to Quality Summary for: [Edition2A](#) | [Edition2-VIRSONly](#) | [Edition2A-TransOps](#) | [Edition2B](#) | [Edition2B-TransOps](#)